ISSN: 2277-9655
Scientific Journal Impact Factor: 3.449
(ISRA), Impact Factor: 1.852

IJESRT

INTERNATIONAL JOURNAL OF ENGINEERING SCIENCES & RESEARCH TECHNOLOGY

Morpho-structural properties of CeO_2 and (CeO_2-CaO, CeO_2-ZnO) Binary Nanostructured Oxides Prepared by the Electrodeposition Method

M. El Hajji[1], A. Hallaoui[1], L. Bazzi[1]*, O. Jbara[2], A. Benlhachemi[1], A. Tara[2], B.Bakiz[1]

[1] Material and Environment Laboratory (LME), Faculty of Sciences, Agadir, Morocco.

[2] Engineering and Materials Science Laboratory (LISM), UFR Sciences, University of Reims, France.

l.bazzi@uiz.ac.ma

Abstract

Ceria thin films (CeO_2) were prepared by electrochemical cathodic deposition process. Different types of substrates were used such as aluminum, titanium and stainless steel. As it is possible to deposit separately pure ceria (CeO_2), pure calcium oxide (CaO) and pure Zinc oxide (ZnO), CeO_2-CaO and CeO_2-ZnO binary oxides thin films were successfully obtained in one electrochemical condition set. By varying the current density, deposition time and electrolyte concentration, the amount of the electrodeposited material could be controlled. The deposits were studied by X-ray diffraction (XRD) and scanning electron microscopy « SEM » coupled to energy dispersive spectrometry « EDS »

Keywords: Electrochemical Cathodic Deposition, CeO_2, CeO_2-CaO, CeO_2-ZnO, X-ray diffraction, SEM, EDS.

Introduction

Nowadays, nanostructured metal oxides are subject of a tremendous attention because of their electronic and optical properties as well as their potential applications; especially in sensors, catalysts, for protection against corrosion, and in electrochemical degradation of waste waters [1-7]. Among the most active rare-earth oxides, ceria has attracted much interest owing to its unique properties including high mechanical strength, oxygen ion conductivity, and oxygen storage capacity. Cerium oxide (CeO2) has been employed as catalyst [8], catalyst support [9,10], for the development of biosensors [11], and in solid fuel electrolyte industries [12]. Ceria thin films have been prepared with different processes such as ion beam deposition [13-16], chemical vapor deposition [17-21], sputtering [22,23], pulsed laser deposition/ablation [24,25], and sol–gel process [26,27]. The electrochemical deposition process has been claimed to become an important method on the processing of this oxide because of the low cost of equipment, also, the films can be obtained on a vast variety of substrates [28-31]. By means of electrodeposition, the morphology and size of metal-oxide crystals are easily controlled by variation in the potential, current density, and concentration of the reactant.

The aim of this study is therefore to elaborate and to characterize the films of pure cerium oxide and nanocomposite cerium binary oxides CeO2-CaO and CeO2-ZnO electrodeposited from precursor using a classic three-electrode cell. The correlation between the electrochemical deposition and the characteristics of the films developed on three kinds of substrates was established through chronopotentiometry experiments, X-ray diffraction « XRD » and scanning electron microscopy « SEM » coupled to energy dispersive spectrometry « EDS ».

Materials and methods

All chemicals used to prepare the thin films, were purchased from Sigma Aldrich. The electrochemical cell used for electrodeposition had been described elsewhere **[32]**. Stainless steel (SS), aluminum (Al) and titanium (Ti) substrates were used as working electrode. Prior to the deposition, substrates were polished mechanically using a mechanical polishing machine on a paper of polishing SiC 600, 800 and SiC 1200 for the completion. Then, the substrates were washed thoroughly with distilled water, rinsed with acetone, and cleaned with ethanol. Finally, they were dried with pulsed hot air immediately before the deposition. XRD analysis was carried out using a BURKER SIEMENS D5000, with Cu Kα1 source (λ = 1.5406 Å) at a glancing angle of 0.5°. To study the surface morphology of obtained films, SEM observation was carried out using Philips XL 30 ESEM-Field-Emission Gun.

ISSN: 2277-9655
Scientific Journal Impact Factor: 3.449
(ISRA), Impact Factor: 1.852

Electrodeposition of cerium oxide

Electrochemical deposition experiments were performed from aqueous solution of cerium nitrate 0.1M «$Ce(NO_3)_3$,6 H_2O » 99%, in galvanostatic regime without stirring and at room temperature. The cathodic deposition at current densities ranging from 1 to 3 $mA.cm^{-2}$ was investigated. The pH was about 3.6. After electrodeposition, the samples were rinsed in ethanol and placed in a desiccator before any further subsequent analysis. Deposit weights were obtained by weighing the substrates before and after deposition experiments.

Electrodeposition of CeO_2-CaO

CeO_2-CaO was electrodeposited using the following chemical products: 0.05 M cerium nitrate; $Ce(NO_3)_3$•$6H_2O$; like cerium precursor, 0.0125 M calcium nitrate; $Ca(NO_3)_2$; like calcium precursor, and 0.1 M potassium nitrate « KNO_3 » like electrolyte support. The electrodeposition was realized using a classical three-electrode experimental set-up **[32]**, with the stainless steel sample being the cathode. The pH of the electrolytic bath was 4.6, and the used cathodic current density was $3.5mA/cm^2$.

Electrodeposition of CeO_2-ZnO

In this part only stainless steel substrate was used as working electrode. To prepare the thin films of CeO_2-ZnO nanocomposite, the following chemical products used were: 0.025M zinc nitrate; $Zn(NO_3)_2$•$6H_2O$; like zinc precursor, 0.1M cerium nitrate; $Ce(NO_3)_3$,$6H_2O$; like cerium precursor, and 0.5M potassium nitrate « KNO_3 » like electrolyte support. The deposition experiments were carried out in the galvanostatic mode without stirring the solution, at room temperature, and the used current density was $2.5mA/cm^2$.

Results and discussion

Electrochemical deposition of Ceria:

Electrochemical mechanism:
The electrochemical mechanism of deposition was largely discussed in the literature [33,34]. Two steps must be distinguished. The first step corresponds to the cathodic generation of ions hydroxyl OH- by the reduction of O_2, H_2O or NO_3^-.

$$O_2 + 2H_2O + 4e^- <====> 4OH^- \quad (1)$$

$$2H_2O + 2e^- <====> H_2\,(g) + 2OH^- \quad (2)$$

$$NO_3^- + H_2O + 2e^- <====> NO_2^- + 2OH^- \quad (3)$$

The second step corresponds to the reaction of precipitation of cerium hydroxide. The formation of hydroxyl ions leads to the local increase of pH on the surface followed by the formation of a precipitate $Ce(OH)_3$ [35].

$$Ce^{3+} + 3OH^- \rightarrow Ce(OH)_3 \quad (4)$$

Then, cerium oxide thin film is formed from the oxidation of Ce(OH)3 (Eq.(5)).

$$Ce(OH)_3 <====> CeO_2 + H_3O^+ + e^- \quad (5)$$

Ceria electrochemical mechanism is really complicated. Li and Thompson [36] suggested that the deposition of the film is preceded by nucleation and a process of growth. For more cathodic current densities, a quick and monotonous decrease of potential is observed in the first few seconds followed by a stabilization of the potential. Such stabilization appears sooner by increasing the applied current density. However, at less current density (lower than or 0.5mAcm−2), the electrodeposition passes by several stages before the potential stabilizes and the obtained film is not homogenous and it contains several cracks [37]. Figure. 1 gives the variation of potential versus time during deposition. In order to obtain homogeneous and less to free crack thin film, the applied current density was about 3mA/cm2. A continuous variation of potential with time is indicative of a single reaction, whereas sudden changes are indicative of a change in the dominant reaction taking place at the electrode.

The chronopotentiometric curve related to CeO_2 film exhibit a particular shape.

ISSN: 2277-9655
Scientific Journal Impact Factor: 3.449
(ISRA), Impact Factor: 1.852

Actually, upon the application of the current density, the cathodic potential increases, as the formation of ceria hydroxide occurs. Over the first 200 s, the potential decreases and reaches the value of about 1520 mV. The second part of the process was characterized by constant potential. This part of process was assigned to the homogenous crystal growths. In this case, only reaction responsible for electrogeneration of OH- is related to the hydrogen evolution reactions. In the initial stage of deposition, the nucleation and the growth of nuclei compete with each other. In the case of high current density "more than 2mA/cm^2", the generation reaction rate is high, and the rate of nucleation exceeds that of growth of nuclei. The first period (t < 2000 s) is attributed to the formation of a deposit of fine particle size that fully covers the surface. Therefore, the potential stabilizes rapidly. It can be related to the stacking of new layers.

The deposit weight was determined according to Faraday's law. Electrolytic deposition experiments revealed the formation of cathodic deposits from cerium nitrate solutions. Figure.2 shows the deposit weight as a function of deposition time for 0.1 M Ce(NO3)3,6 H2O solution. Lower deposit weights were obtained at lower deposition time. It should be noted that in low concentration of electrolytes the rate of hydrolysis reactions depends on the rate of diffusion of the reacting species, detracting from the deposition process efficiency. Globally, nearly linear dependence was observed.

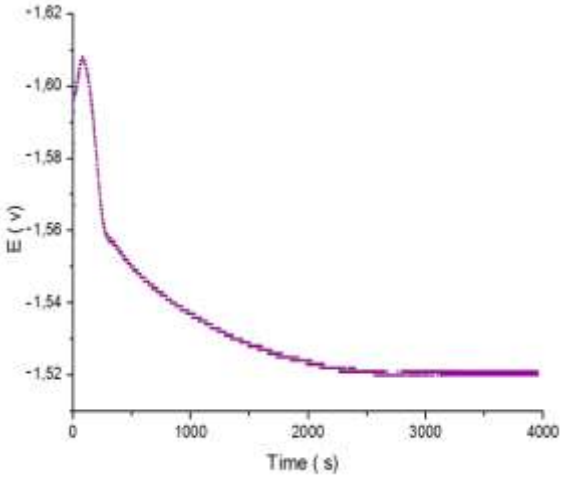

Figure.1. Evolution of potential with deposition time in 0.1M Ce(III) nitrate solutions, 3 mA.cm^{-2} and at room temperature.

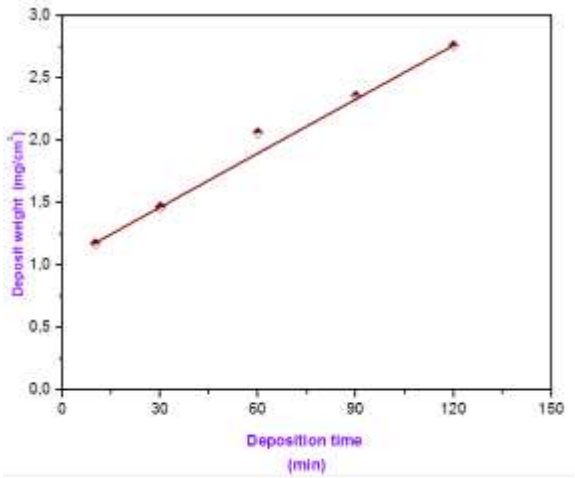

Figure. 2. Deposit weight vs. deposition time for deposits obtained from 0.1 M cerium nitrate solution at a current density of 3mA/cm^2.

Characterization of the deposits

The XRD studies were carried out on CeO_2 in order to determine phase and crystallographic analysis. All obtained XRD patterns were analyzed using the X'Pert HighScore software. Typical X-ray diffractogram of electrodeposited CeO_2 onto aluminum (Al) substrate is shown in figure 3.

The peaks located at 2θ = 28.31°, 32.96°, 47.56° and 56.31° could be related to the (111), (200), (220) and (311) reflections of the cerium oxide species, respectively. They are generally less intense compared to Al peaks. According to JCPDS 43-1002, the registered peaks clearly confirm that the cubic fluorite CeO_2 phase is the compound diffracting from the thin film. As observed from the figure 3 that, XRD peak (111) is the more dominant against others.

To study the effect of changing the substrate, we had electrodeposited CeO_2 onto SS and Ti substrates, respectively. The results are shown in figure 4 and 5.

ISSN: 2277-9655
Scientific Journal Impact Factor: 3.449
(ISRA), Impact Factor: 1.852

From figure.4, The XRD pattern shows the material to be polycrystalline and a strongest peak corresponding to the (111) plane appeared. Contrary to figure.3, the peaks related to SS substrate are less intense.

In figure.5, the XRD patterns of electrodeposited CeO_2 onto Ti substrate are displayed. Generally, diffraction lines of both films can be indexed as CeO_2 structure. Diffraction peaks match well with the peaks of cubic fluorite CeO_2 crystal structure. The broadening of the diffraction peaks indicates the formation of nanocrystals. As observed, XRD peak (111) located at $2\theta = 28.5°$ is the dominant one in all patterns. Lower intensity peaks, also detected in the patterns at the following 2θ values of 33°, 47.6°, 56.3°, are assigned to (200), (220) and (311) crystallographic planes, respectively. With the appearance of the new peaks corresponding to the (222) "Figure.4" and (331) "Figure 5" planes, matching to ceria.

Table.1. shows the calculated average size of the crystallites of electrodeposited CeO_2 onto SS , Al and Ti substrates. The grain sizes estimated from the X-ray diffraction peak width, using Scherrer's formula [38] were between 17 and 23 nm. This result confirms the good crystallinity of the samples and the nanometric size of crystallites.

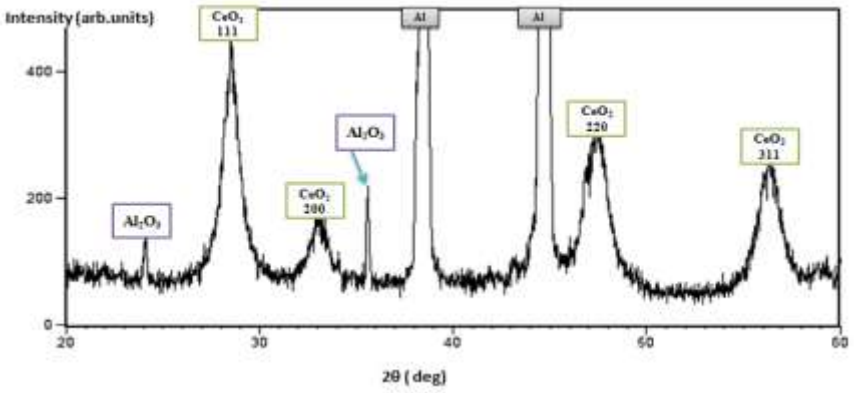

Figure. 3. XRD patterns of nanostructured CeO_2 films electrodeposited on Al substrate

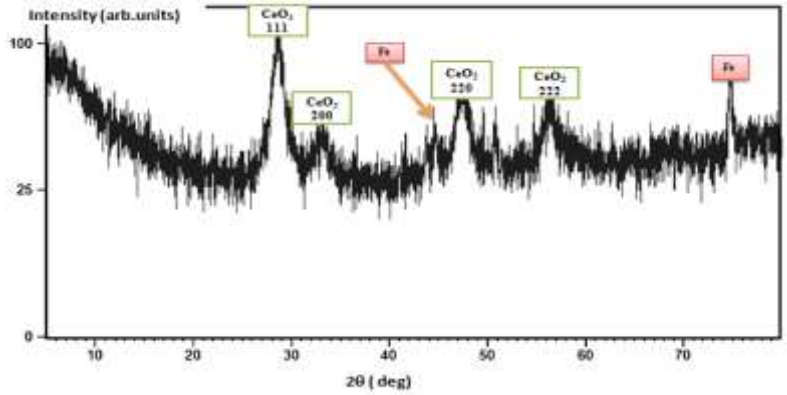

Figure. 4. XRD patterns of nanostructured CeO_2 films electrodeposited on SS substrate

ISSN: 2277-9655
Scientific Journal Impact Factor: 3.449
(ISRA), Impact Factor: 1.852

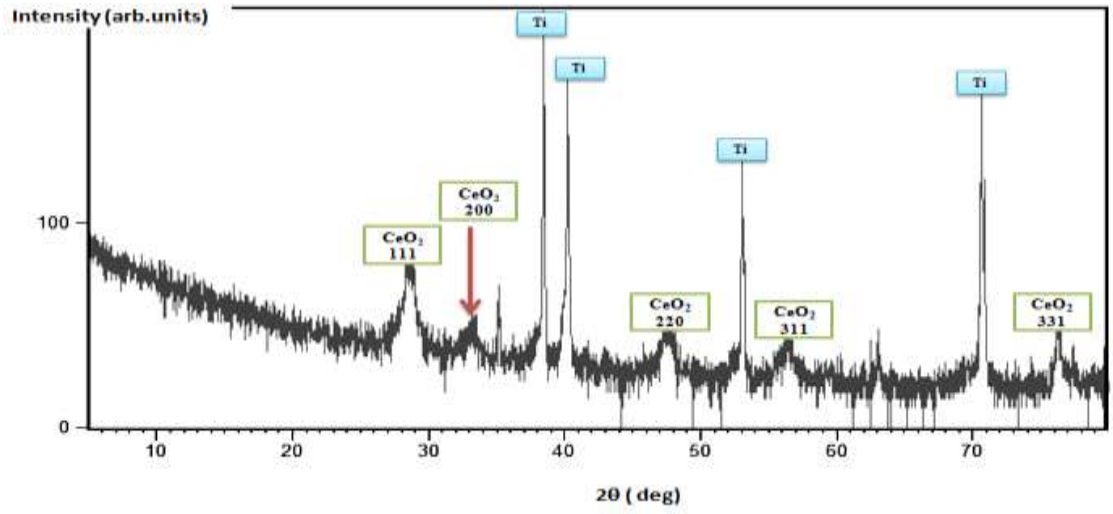

Figure. 5. XRD patterns of nanostructured CeO_2 films electrodeposited on Ti substrate

Table.1. : Average grain size of CeO_2 calculated by the Scherrer's equation

Substrate	Crystallites size (nm)
Ti	21.7
SS	23.3
Al	17.5

SEM observation was used to investigate the surface morphology. Figure.6 illustrates the appearance of the electrodeposited CeO_2 onto Al substrate showing homogeneous and void-free surface. It can be seen that the films fully covers the surface of the substrate. Figure.7 shows the SEM images of the CeO_2 deposit obtained using different magnification. Generally, the products were observed as nanostructures with diameters of a few tens of nanometers on the substrate. The length of nanostructures is up to a few micrometers. The film exhibits some cracks (figure.7a). Figure.7b allows us to view that the layers obtained had a specific morphology. The enlarging of a grain makes it possible to visualize the layer covered with small fine grains like the hair shapes (Figure.7c). SEM provides information not only on morphology, the distribution and the size of the grains or the agglomerates, but also on the local chemical composition when it is coupled with EDS X-Ray spectrometer. Figure.8 shows the results obtained by EDS X-Ray analysis of pure ceria. The EDS analysis confirms the presence of oxygen, and cerium elements in the deposit. The weight elements percentage was close of the nominal composition. Figure.8. EDS spectrum related to the deposit of the pure cerium oxide. The SEM image (A) indicates the zone where the spectrum is acquired. The inserted table indicates the weight percents of ceria elements.

ISSN: 2277-9655
Scientific Journal Impact Factor: 3.449
(ISRA), Impact Factor: 1.852

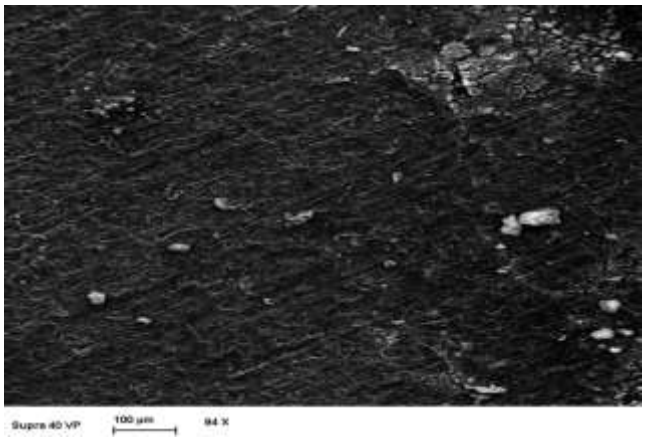

Figure.6. SEM micrograph of electrodeposited CeO_2 on Al substrate

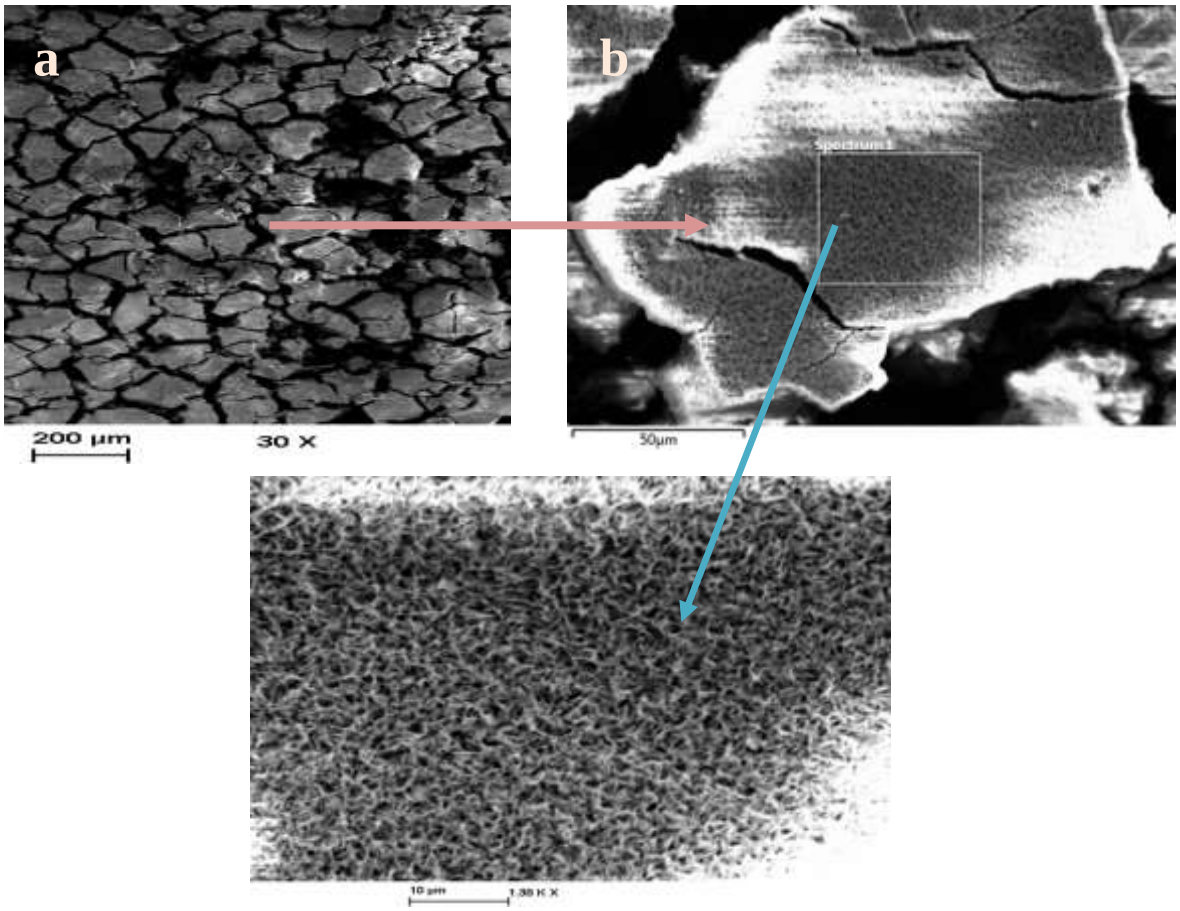

Figure.7. Typical SEM images of thin films grown on Al substrate at different magnifications

ISSN: 2277-9655
Scientific Journal Impact Factor: 3.449
(ISRA), Impact Factor: 1.852

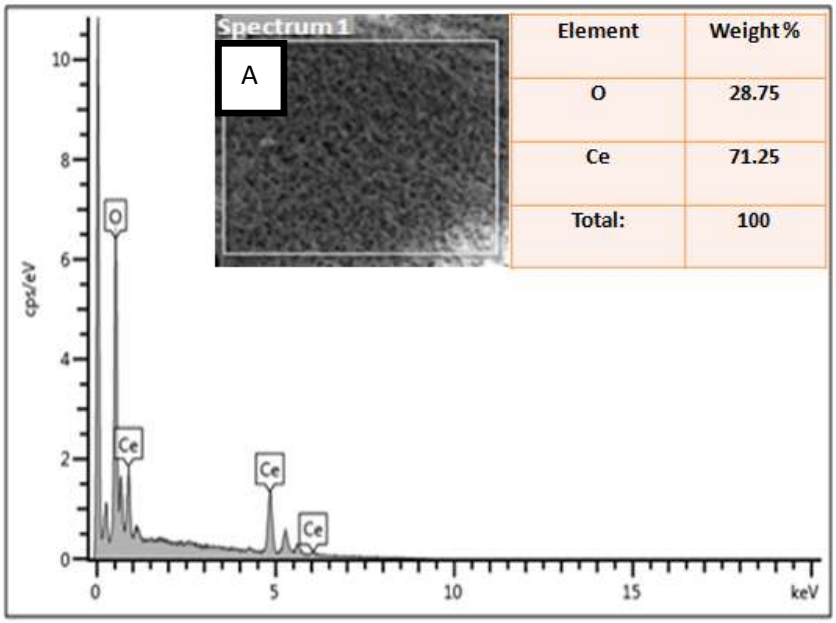

Figure.8. EDS spectrum related to the deposit of the pure cerium oxide.

As we had already noted that, the cathodic deposition of ceria was made onto three different substrates such titanium, aluminum, and stainless steel. It is important to note that deposits of the similar microstructure were obtained on these various metal surfaces.

Figure.9. illustrates the SEM micrographics of the electrodeposited pure CeO_2 thin film. Although both films fully cover the substrate, it is easy to observe that the thin film of ceria electrodeposited on SS and Ti exhibit the same morphology on Al (figure.7). This result is confirmed in Figure.10 (a and b). It represents the magnifications of two zones: (left) the enlargement of an area of CeO_2 deposited on SS, and on Ti (right).

Globally, electrodeposited ceria thin films have a smooth surface and exhibit a close morphology independent on the substrate used. The Al substrate gives rise to dense ceria thin films-based on hair shaped nanoparticles. On the other hand, ceria exhibits a close structure when grown on the Ti and SS substrates. A magnified image shows that it is composed of even smaller, tiny, interconnected nanoparticles like needle. From the SEM graph some cracks marked significantly the structure. Especially, on stainless steel and titanium substrate, extensive cracking can be seen on the film surface. These cracks are associated with either the formation of gas bubbles during the process on the substrate surface, to the dehydration process itself, to a large mismatch between the substrate and film, or drying process [39]. EDS X-Ray analysis confirms the presence of oxygen, and cerium elements in the deposit. Also, the XRD patterns confirm that the cubic fluorite CeO_2 phase is the major compound diffracting from the deposits. No diffraction line associated with Ce (III) hydroxide is present. Likewise, no broad spot appears. Normally, this spot is coupled to the carbonation of the ceria films which can be responsible for the formation of the green rust. It is associated to the corrosion, especially, on the stainless steel substrate. These results have been confirmed by SEM/EDS analysis.

ISSN: 2277-9655
Scientific Journal Impact Factor: 3.449
(ISRA), Impact Factor: 1.852

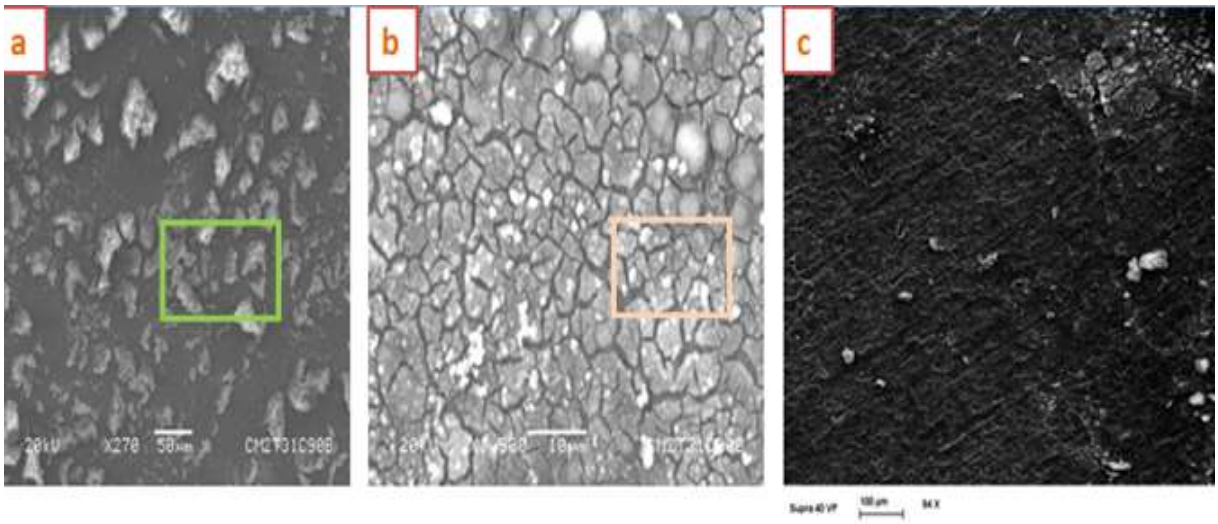

Figure 9. SEM micrographics of the electrodeposited pure CeO_2 thin film on (a) Ti (b) SS and (c) Al substrates.

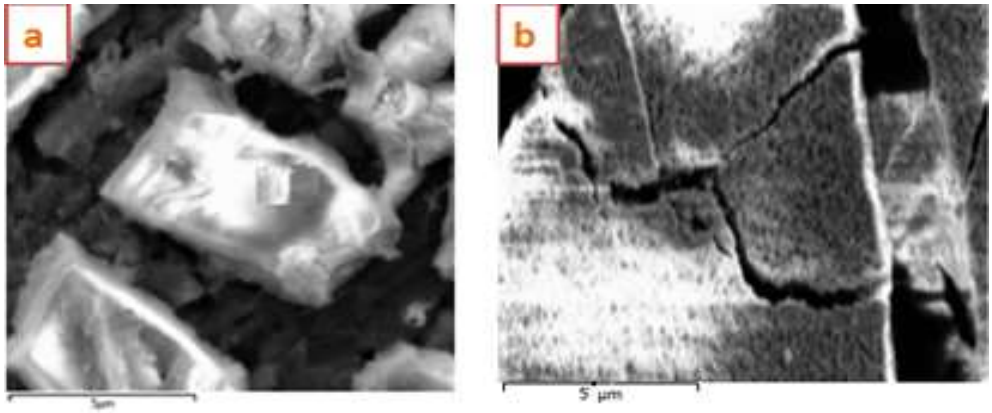

Figure.10. SEM micrographics for the deposits a zoom of boxed area of CeO_2: (right) on Ti and (left) on SS

Electrochemical deposition of CeO_2-CaO

Crystal Structure

The crystallographic structures of CeO_2-CaO are deduced from XRD patterns presented in Figure.11. The CeO_2 is a random pattern with typical FCC fluorite structure and the reflection assignment detail is discussed in the first paragraph.

The electrosynthesized CeO_2-CaO composite retain the FCC fluorite structure characteristic of CeO_2. Also, XRD patterns of CeO_2-CaO indicate that as-produced cerium oxide is randomly ordered and participation of CaO in reaction has no influence in orientation of structure. The particle sizes of CeO_2-CaO were estimated from the FWHM of CeO_2 (111) reflection by using Scherrer equation [38] and listed in Table.2. The product is in nanoscale, which qualifies as-produced composites being called nanocomposite. Compared with pure cerium oxide thin film made using the same approach and on the same condition, cerium oxide particle in the nanocomposite exhibits larger size (Table.2). The

ISSN: 2277-9655
Scientific Journal Impact Factor: 3.449
(ISRA), Impact Factor: 1.852

peaks of cerium and calcium oxides are confused at $2\theta = 28°$, and no diffraction line associated with hydroxide is present.

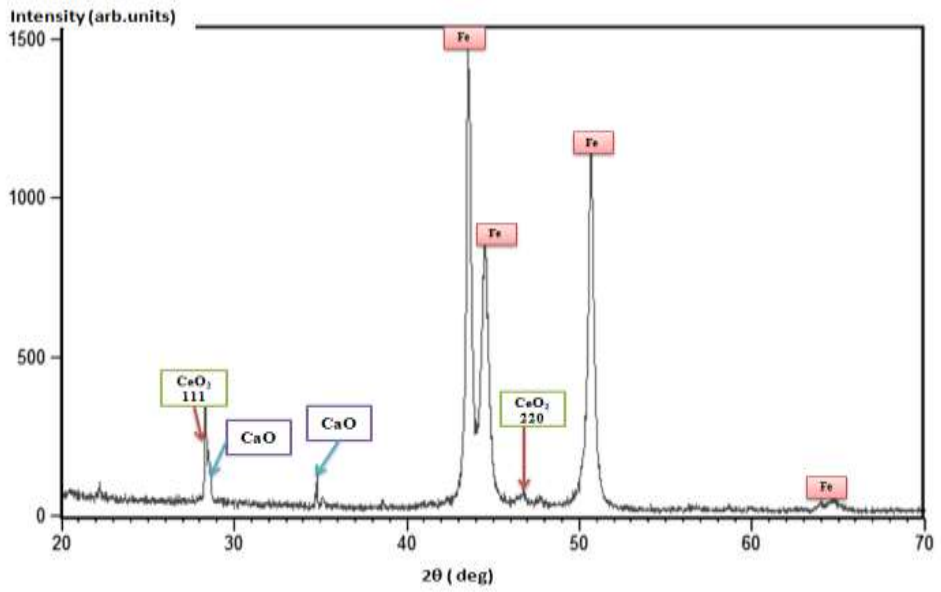

Figure.11. XRD patterns for CeO_2-CaO nanocomposite oxide

Table.2. CeO_2 Particle size vs. content of CaO in nanocomposite

Samples	SS/Ceria (Fig.4)	SS/CeO_2-CaO (Fig.11)
Reflection	28.31	28.59
Particle size (nm)	39.4	74.2

ISSN: 2277-9655
Scientific Journal Impact Factor: 3.449
(ISRA), Impact Factor: 1.852

Surface Morphologies of Films

The morphologies of as-formed nanocomposite oxides were examined using scanning electron microscopy "SEM ". Fig.12 shows the appearance of the electrodeposited CeO_2-CaO onto stainless steel substrate showing homogeneous and cracking surface. Figure.13 illustrates the selected SEM pictures of the CeO_2-CaO composite films obtained using different magnification. Since, CaO oxide is more readily to interact with the cerium oxide system in an aqueous reaction environment, which can be verified in the morphology of the films. The CeO_2-CaO nanocomposite, at a certain content of calcium, gives a homogenous surface with the calcium incorporated with the cerium oxide surface. As predicted, the galvanostatic deposition mode with applied current –3.5mA/cm^2 at 30oC (room temperature) leads to more CeO_2 (111) preferred structure (figure 11). The enlarging of a zone (figure 13) makes it possible to visualize a cluster of grains of micrometric size. The usual form of the cerium oxide is observed. However, on the film surface some cracks appears but they are less significant compared with the ceria (figure.7a). As discussed in the literature [40], these cracks are associated with either the formation of gas bubbles, to the dehydratation process itself or from the shearing stress between the substrate and the deposit. In this case, the second proposal remains most probable. EDX on cross-section and surface of CeO_2-CaO nanocomposite films reveals presence of elemental Ce, Ca, and O in the nanocomposite films (figure 14). Among those, Fe and K are attributed to stainless steel substrate.

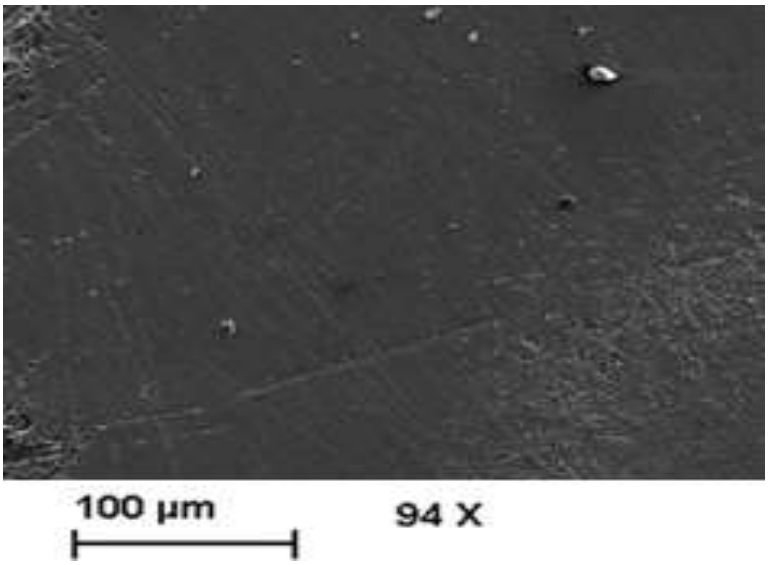

Figure.12. SEM micrograph of electrodeposited CeO_2-CaO

ISSN: 2277-9655
Scientific Journal Impact Factor: 3.449
(ISRA), Impact Factor: 1.852

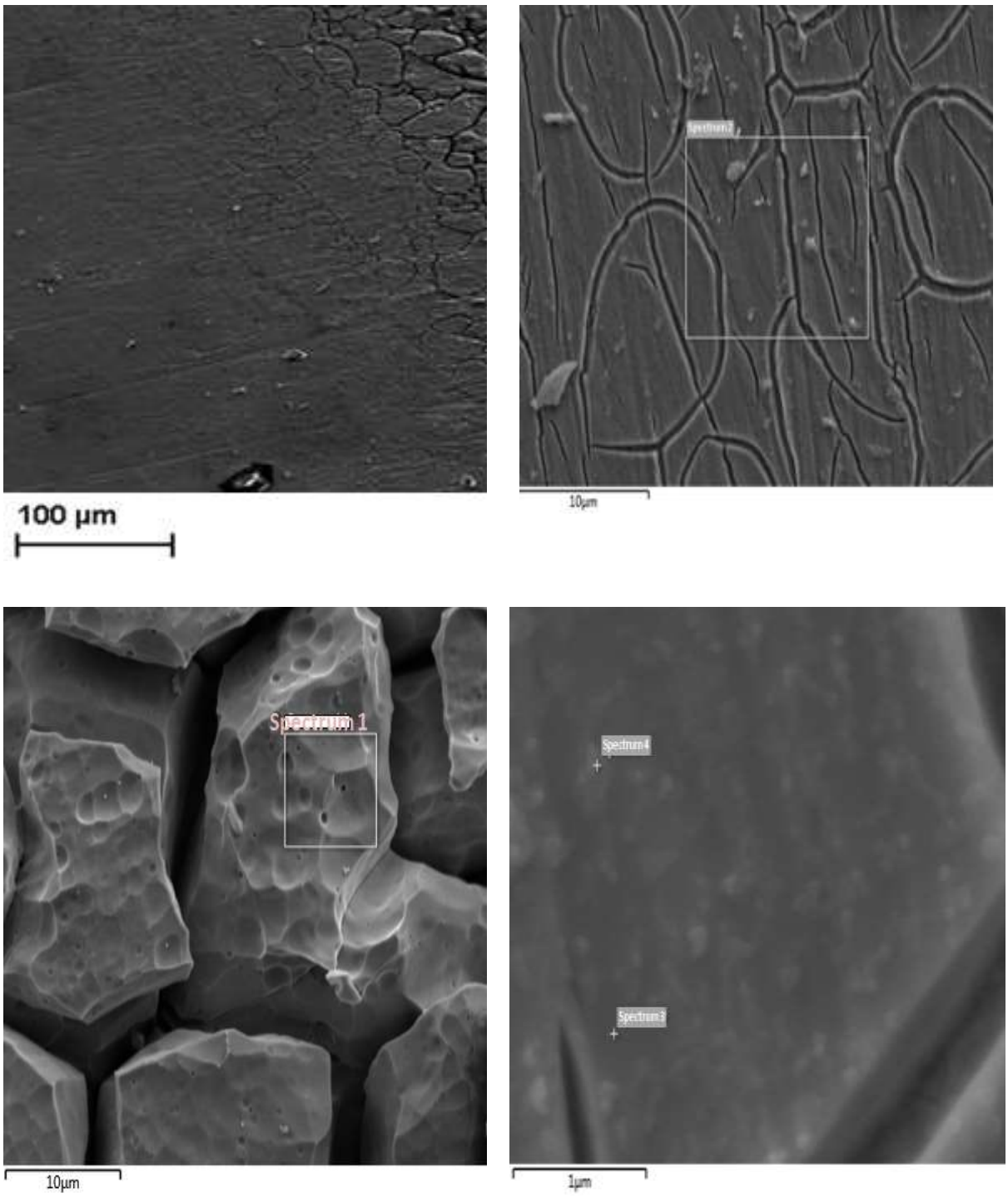

Figure.13. Typical SEM images of thin films grown on SS substrate at different magnifications.

ISSN: 2277-9655
Scientific Journal Impact Factor: 3.449
(ISRA), Impact Factor: 1.852

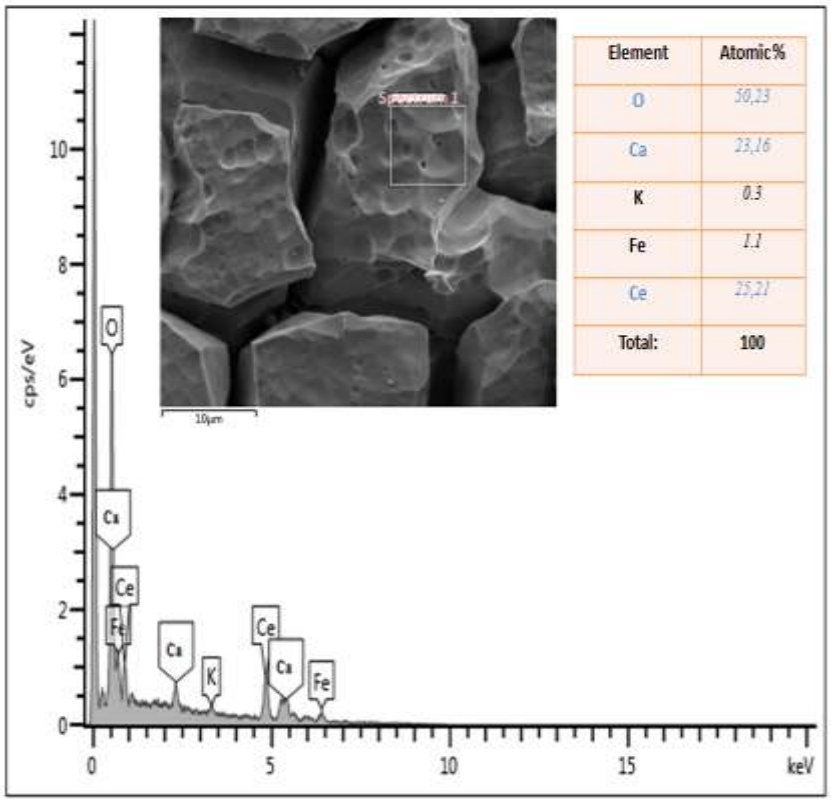

Figure.14. EDS spectrum related to the deposit of CeO_2-CaO.

Electrochemical deposition of CeO_2-ZnO: Crystal Structure and Surface Morphologies of Films

The preliminary studies on CeO_2-ZnO based nanocomposite indicate that ZnO incorporated into ceria film can result in more homogeneous films. The usual galvanostic electrodeposition leads to good adhesion and does not change the basic property of ceria.

Using less current density (2mA/cm^2), XRD patterns of CeO_2-ZnO nanocomposite film indicate that this type of binary oxide demonstrates the same property and trend as other type discussed in previous section. Table.3. lists the particle sizes of nanocomposite leads to a relatively more (200) oriented film (figure 15) with particle size of 32 nm. To validate the incorporation of ZnO within ceria oxide films, both film surface and cross-section were subjected to SEM / EDX detection. The surface (Figure 16) exhibits a thick construction. Under high magnification, the layered structure of CeO_2-ZnO binary oxide can be seen. For this system, the film is quite homogeneous, with no cracks on its surface, and has the same morphology as pure ceria film (Figure.7c). Dispersive X-ray analysis reveals elemental Ce, Zn, and O were present in the film (figure 17).

Table.3. CeO_2 Particle size vs. content of ZnO in nanocomposite

ISSN: 2277-9655
Scientific Journal Impact Factor: 3.449
(ISRA), Impact Factor: 1.852

Samples	**SS/Ceria (Fig.4)**	**SS/CeO_2-ZnO (Fig.15)**
Reflection	*28.31*	*28.59*
Particle size (nm)	*39.4*	*32.2*

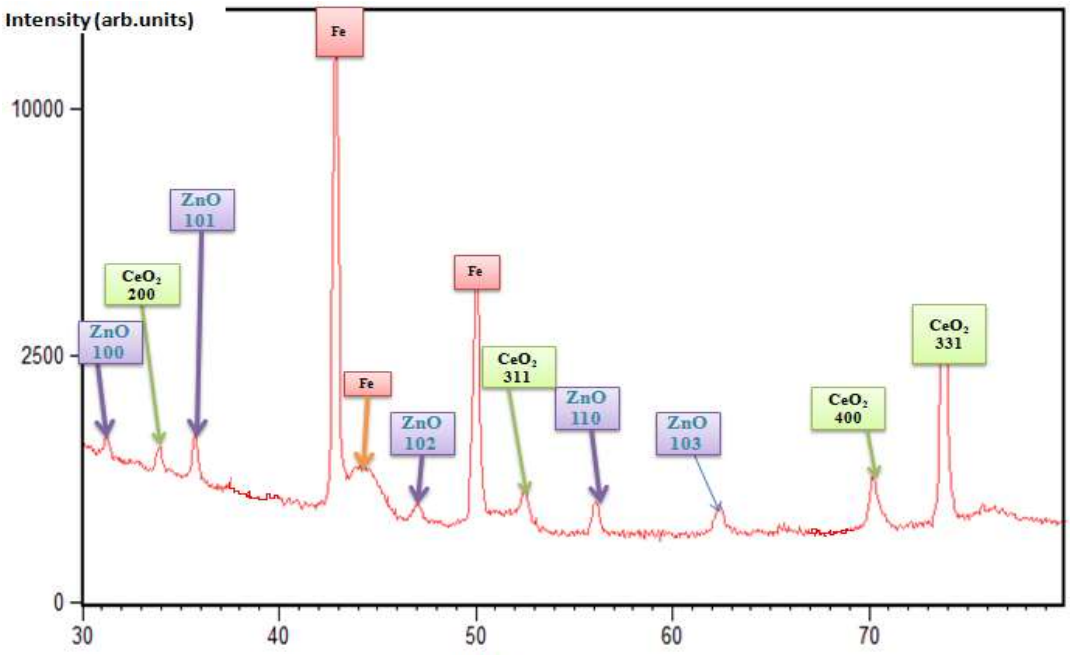

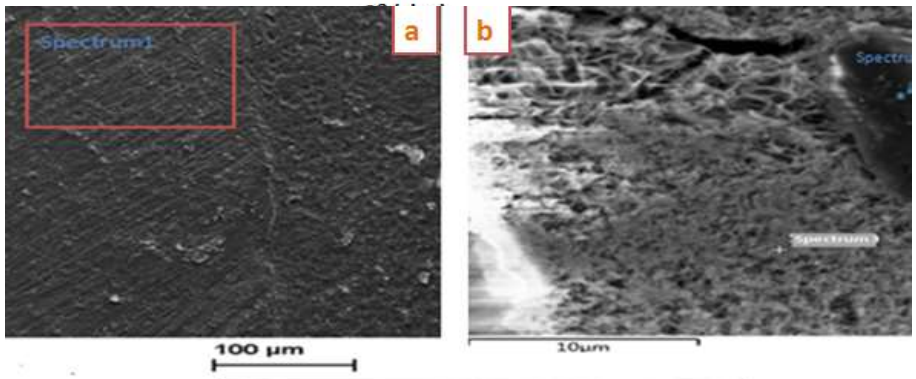

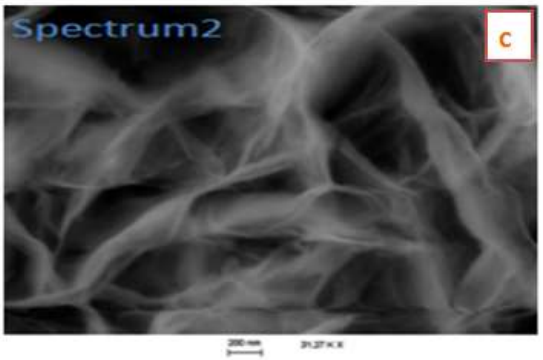

Figure.15. X-ray diffractogram of electrodeposited nanocomposite oxides onto steel substrate. ***CeO_2-ZnO stainless***

ISSN: 2277-9655
Scientific Journal Impact Factor: 3.449
(ISRA), Impact Factor: 1.852

Figure.16. SEM micrographs for the deposits of CeO_2-ZnO and a zoom of boxed area (spectrum 1&2)

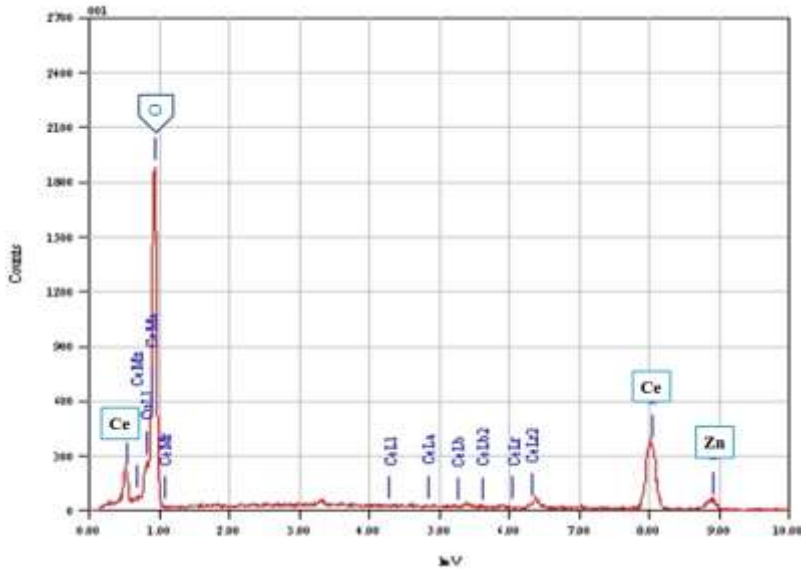

Figure.17. EDS Spectrum of CeO_2-ZnO in the boxed area (Figure.16)

From the results, the cathodic electrodeposition of CeO_2-ZnO was confirmed by all analysis. CeO_2 kept its cubic form. The surface of deposit does not present any network of cracks, which presents a

ISSN: 2277-9655
Scientific Journal Impact Factor: 3.449
(ISRA), Impact Factor: 1.852

promising result. ZnO played an important role in the CeO_2-ZnO system. Normally, ceria had high activity, good stability and may find application in the catalysis field. The elaboration of CeO_2-ZnO nanocomposite oxides can help to increase the catalytic properties of ceria, especially as ZnO was able to overcome the problem of cracking. The electrocatalytic efficiency test of CeO_2-ZnO binary oxide will be investigated.

Conclusion

This study has shown that CeO_2, CeO_2-ZnO and CeO_2-CaO have been successfully produced by means of cathodic electrodeposition method. The deposition process has been quantified in experiments performed with three kinds of substrates. The amount of the deposited material can be controlled by variation of deposition time, current density and electrolyte concentration. The ceria and the binary oxides were synthesized at room temperature, under galvanostatic conditions. All obtained films had a nanocrystalline structure, and close morphology. The results were confirmed by XRD measurement and SEM analysis. Moreover, ZnO was found to contribute to the better crystallinity and no cracks of ceria, this was proven by XRD and SEM analysis.

References

[1] *Y. Sun, N. G. Ndifor-Angwafor, D. J. Riley, and M. N. R. Ashfold, Chem. Phys. Lett. 43. 2006.*
[2] *Y. Gao, M. Nagai, T.-C. Chang, and J.-J. Shyue, Cryst. Growth Des. vol.7. 2007.*
[3] *Y. Masuda, S. Wakamatsu, and K. Koumoto, J. Eur. Ceram. Soc. vol.24. 2004.*
[4] *S. T. Chang, I. C. Leu, and M. H. Hon, J. Cryst. Growth. no.273. 2004.*
[5] *L. Vayssieres and M. Graetzel, Angew. Chem. Int. Ed. 43. 2004. pp. 3666.*
[6] *C. Levêque, Watery Ecosystems (Hachette, 1996).*

[7] *http:// Sagascience@cnrs-dir.fr*

[8] *Shen, W.; Matsumura, Y. Journal of Molecular Catalysis A: Chemical.2000, pp. 165-168.*

[9] *Xavier, K. O.; Sreekala, R.; Rashid, K. K. A.; Yusuff, K. K. M.; Sen, B. Catalysis Today. Vol.49 . 1999, pp. 17-22.*

[10] *Yao, C.; Weng, H. Industrial & Engineering Chemistry Research no.37.1998, pp.2647-2653.*

[11] *K.J. Feng, Y.H. Yang, Z.J. Wang, J.H. Jiang, G.L. Shen, R.Q. Yu, Talanta no.70.2006.*

[12] *H. Inaba and H. Tagawa, Solid State Ionics,1996.*

[13] *Wu, Z.; Huang, D.; Yang, X. Vacuum no.51.1998, pp. 397-401.*

[14] *Gnanarajan, S.; Savvides, N. Thin Solid Films . 1999, pp. 124-129.*
[15] *Cotell, C. M.; Hirvonen, J. K. Surface and Coatings Technology. 1996, pp. 118-124.*
[16] *Huang, D.; Qin, F.; Yao, Z.; Ren, Z.; et.al. Applied Physics Letters .vol.67. 1995, pp.3725-3726.*

[17] *Pan, M.; Meng, G. Y.; Xin, H. W.; Chen, C. S.; et.al. Thin Solid Films. 1998, pp. 89-93.*
[18] *Wang, A.; Belot, J. A.; Tobin, J. M.; Markworth, P. R. Physica C. 1999, pp. 154-160.*
[19] *Pollard, K. D.; Jenkins, H. A.; Puddephatt, R. J. Chemistry of Materials.vol.12. 2000,pp.701-710.*
[20] *Nigro, R. L.; Malandrino, G.; Fragalà, I. L. Chemistry of Materials. 2001, pp. 4402-4404.*
[21] *Carter, W. B.; Book, G. W.; Pollery, T. A.;Stollberg, D. W.; Hampikian, J. M. Thin Solid Films. 1999, pp. 25-30.*

[22] *Chin, C. C.; Lin, R. J.; Yu, Y. C.; Wang, C. W.; et.al. Physica C. 1996, pp. 86-92.*
[23] *Chin, C. C.; Lin, R. J.; Yu, Y. C.; Wang, C. W.; et.al. IEEE Transactions on Applied Superconductivity. Vol.7. 1997, pp. 1403-1406.*
[24] *Amirhaghi, S.; Li, Y. H.; Kilner, J. A.; Boyd, I. A. Materials Science and Engineering. 1995, pp. 192-198.*
[25] *Shi, D. Q.; Ionescu, M.; McKinnon, J.; Dou, S. X. Physica C. 2001, pp. 304-310.*
[26] *Wang, S; Wang, W; Liu, Q.; Zhang, M.; Qian, Y. Solid State Ionics. 2000, pp. 211-215.*
[27] *Czerwinski, F. Szpunar Thin Solid Films. 1996, pp.213-219.*
[28] *Y. Zhou, J.A. Switzer, J. Alloy Compd. pp. 237, 1996.*
[29] *I. Zhitomirsky, A. Petric, Mater. Lett. 1999.*
[30] *I. Zhitomirsky, A. Petric, Ceram. Int. 2001.*
[31] *P. Stefanov, G. Atanasova, D. Stoychev, Ts. Marinova, Surf. Coat. Technol. 2004.*
[32] *M. El Hajji, A. Hallaoui, L. Bazzi, O. Jbara, A. Benlhachemi, A. Tara, B.Bakiz, Int. J. Electrochem. Sci, accepted (2014).*
[33] *M. Balasubramaniana, C.A. Melendresa, A.N. Mansour, Thin Solid Films. 1999, pp. 178.*
[34] *L. Arurault, P. Monsang, J. Salley, R.S. Bes, Thin Solid Films. 2004, pp.75.*

ISSN: 2277-9655
Scientific Journal Impact Factor: 3.449
(ISRA), Impact Factor: 1.852

[35] Y. Hamlaoui, F. Pedraza, C. Remazeilles, S. Cohendoz, C. Rebere, L. Tifouti, J.Creus, Mater. Chem. Phys. 2009, pp. 650.
[36] Li, E.B., Thompson, G.E. Situ atomic force microscopy studies of the deposition of cerium oxide films on regulary corrugated surfaces. J. Electrochem. Soc., vol.146, pp.1809-1815, 1999.
[37] J.O'M. Bockris, G.A. Razumney, Fundamental Aspects of Electrocrystallization, Plenum Press, New York, 1967, pp. 27.
[38] B.D. Cullity, Elements of X-ray Diffraction, 2nd ednR, Addison Wesley. Reading. MA, 1978.
[39] H.Y. Chang, H.I. Chen, J. Cryst. Growth, 2005.
[40] J. Creus, F. Brezault, C. Rébéré, M. Gadouleau, Surf. Coat. Technol, 2006.